CERN-INTC-2021-012 / INTC-P-595
06/01/2021

EUROPEAN ORGANIZATION FOR NUCLEAR RESEARCH

Proposal to the ISOLDE and Neutron Time-of-Flight Committee

Neutron single-particle states and neutron-capture cross sections towards ^{78}Ni: ^{79}Zn$(d,p)^{80}$Zn

January 6, 2021

E. Sahin[1], G. de Angelis[2] K.S. Beckmann[1], F. Bello[1], H.C. Berg[3] T.K. Eriksen[1], D. Gjestvang[1], A. Görgen[1], M. Guttormsen[1], K. Hadyńska-Klęk[4], V. W. Ingeberg[1], P. Jones[5], A.C.Larsen[1], K.L.Malatji[5], M. Markova[1], W. Paulsen[1], L.G. Pedersen[1], L.Pellegri[5], S. Siem[1], M. Wiedeking[5], F.Zeiser[1] and TREX and MINIBALL collaborations.

[1] *University of Oslo, Oslo, Norway*
[2] *INFN Laboratori Nazionali di Legnaro, Italy*
[3] *Michigan State University, East Lansing, Michigan, USA*
[4] *Heavy Ion Laboratory, University of Warsaw, Poland*
[5] *iThemba LABS, South Africa*

Spokesperson: E. Sahin eda.sahin@fys.uio.no
Contact person: Karl Johnston karl.johnston@cern.ch

Abstract: The aim of the present proposal is to study neutron single-particle energies of the neutron-rich ^{80}Zn nucleus via one-neutron pickup reaction in inverse kinematics, ^{79}Zn(d,p) ^{80}Zn. ^{80}Zn is the most exotic $N = 50$ isotone towards $Z = 28$. The high-lying neutron core excited states will be populated and identified by spin and parity for the first time through the proposed one-step direct reaction process. The ^{79}Zn beam at an energy of 5.5 MeV/A will be impinging on a deuterated-polyethylene target. Emitted protons as well as γ rays de-exciting the states in the residual nucleus will be detected using the MINIBALL + T-REX setup. ^{80}Zn is also an important nucleus for the weak r-process and the present reaction and the setup will allow us to study the statistical properties of the quasi-continuum states and to constrain the (n,γ) cross section for the first time in the proposed experiment. In order to increase the statistics of the γ rays at higher energies, 6 $LaBr_3$ detectors from the University of Oslo will be installed.

Requested shifts: 18 shifts for the ^{79}Zn beam plus 3 shifts to optimize the production and purification of the beam.
Installation: MINIBALL + T-REX + 6 $LaBr_3$ detectors from Oslo

1 Motivation

The motivation is divided into two main objectives and will be discussed in the following. The data obtained in the present work will be analysed using two different methods, thus will form the basis for two separate PhD projects.

1.1 Evolution of the $N = 50$ shell gap

The first objective of the proposal will be dedicated to exploring the evolution of the neutron $N = 50$ shell gap towards ^{78}Ni. The evolution of the $N = 50$ shell closure comprises the nuclei from $Z = 40$ (^{90}Zr) to $Z = 28$ (^{78}Ni) along the $N = 50$ isotonic chain. From the shell model point of view, the evolution of the $N = 50$ gap is primarily due to the monopole tensor interaction: With decreasing number of protons in the fp-shell orbitals ($1f_{7/2}$, $2p_{3/2}$,$1f_{5/2}$, $2p_{1/2}$) the neutron single-particle energies forming the $N = 50$ shell gap will be shifted and even an inversion between the $\nu 1g_{7/2}$ and $\nu 2d_{5/2}$ orbitals may occur. [1, 2] The present study proposes to determine the size of the gap and changes in the effective single-particle energies via neutron excitations above the $N = 50$ shell gap, i.e. between $\nu 2d_{5/2}$ and the $\nu 1g_{9/2}$. Identification of the excited states due to these $1p-1h$ intruder configurations in $N = 50$ isotones gives the direct knowledge of the evolution of the $N = 50$ gap and the single-particle orbitals.

The calculated wave functions for the particle-hole ($np - nh$, n=1,2,3,4 at most) excitations above the $N = 50$ shell gap show a presence of a significant component of $1p - 1h$ excitation with the ($\nu 1g^{-1}_{9/2} \otimes \nu 2d^{1}_{5/2}$) configuration [3]. The resulting states arising from the ($\nu 1g^{-1}_{9/2} \otimes \nu 2d^{1}_{5/2}$) configuration form a multiplet with J^{π}=2^+, 3^+, 4^+, 5^+, 6^+, 7^+. A complete identification of these multiplets along the $N = 50$ isotonic chain has been done for $^{90}_{40}$Zr and $^{88}_{38}$Sr so far via one-neutron pickup reactions, ^{91}Zr(^{3}He,α)^{90}Zr and ^{87}Sr(d,p)^{88}Sr, respectively [4, 5]. Starting from $^{86}_{36}$Kr, the multiplet was only partially identified [6].

The $^{82}_{32}$Ge nucleus is the last member of the chain where only the 5^+ and 6^+ states could be identified as the $1p - 1h$ multiplets, when compared to the shell model calculations [3]. Furthermore, a shell gap value of 4.7 MeV at Z=28 (^{78}Ni) and 3.6 MeV for ^{82}Ge was estimated in the same work. Similarly, large scale shell-model (LSSM) calculations using larger model space, mainly pf-shell orbitals for protons and $f_{5/2}$, p, $g_{9/2}$, and $d_{5/2}$ orbitals for neutrons concluded that neutron excitations above the N=50 gap are important in order to understand changes in the neutron effective single-particle energies [7]. The calculations predicted a minimum at $Z = 32$ and increase towards $Z = 28$ as expected.

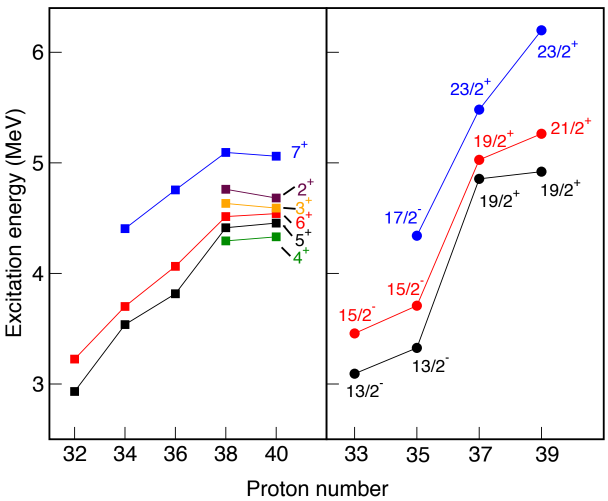

Figure 1: Evolution of the $1p - 1h$ excited states in the even-even and even-odd $N = 50$ isotones.

Presently, ^{80}Zn is the most exotic member along the $N = 50$ chain for which spectroscopy is now accessible at ISOLDE. The present proposal, therefore, aims at studying neutron single-particle energies of ^{80}Zn via the (d, p) reaction in inverse kinematics. The states from the $1p - 1h$ excitations to $2d_{5/2}$ (i.e. 2^+,3^+,4^+,5^+,6^+, and 7^+) and to $3s_{1/2}$ (i.e. 4^+,5^+) and thus the evolution of the $N = 50$ gap up to $Z = 30$ will be determined in a very selective way. This study will help us to understand the role of the correlations and greatly contribute to increase our knowledge on the $p - n$ interactions, in particular the contribution of the tensor interaction between the involved shells in the ^{78}Ni mass region.

1.2 Weak r-process around the A∼80 mass region

The second objective of the proposal is related to the statistical properties of the ^{80}Zn nucleus relevant to the r-process calculations. ^{80}Zn is believed to be one of the three most prominent waiting-point nuclei (together with ^{130}Cd and ^{195}Tm), responsible for the increased abundance observed at mass numbers 80, 130 and 195. They are particularly important since they serve as critical normalization points to constrain the conditions required to describe a realistic rapid neutron capture process (r-process) [8]. The waiting-point theory was later supported by the experimental data such as β-decay half life [9] as well as neutron-separation energy and neutron-capture Q-value [10].

In addition to r-process, spectroscopic studies of some very metal-poor stars in the Galactic halo suggested another process, the so-called weak r-process, to be responsible for the formation of lighter nuclei with A $<$ 130 [11, 12]. Surman et al. [13], performed a sensitivity study of the neutron capture reaction in the context of the weak r-process that forms primarily the A $\sim$ 80 r-process peak [13, 14] (see Figure 2). A wide range of neutron-rich nuclei below, at, and beyond $N = 50$ closed shell are predicted to be sensitive to the neutron capture (n-capture) process from winds occurring in supernovae or collapsar accreditation disks [15, 16]. ^{80}Zn is among these nuclei with larger sensitivity to the neutron-capture cross section and will be the second objective of the presented proposal.

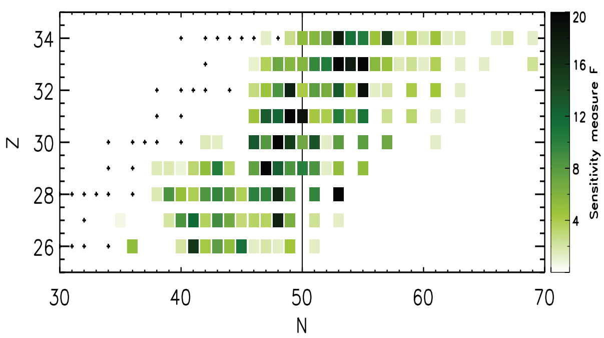

Figure 2: Fifty-five neutron capture rate sensitivity studies. The shading indicates the maximum sensitivity measure F obtained in the full set of sensitivity studies, with the darkest squares indicating maximum F measures of greater than 20. Figure is taken from Ref. [13].

Statistical properties of the atomic nucleus are described by nuclear level density (NLD) and gamma strength function (gSF). Here, the NLD is the total number of states accessible in a given excitation energy and the gSF is the probability that a γ ray of a certain energy will be emitted from an excited nucleus. The so-called Oslo Method will be used to extract these quantities. The Oslo-method is a statistical experimental method for the simultaneous extraction of NLD and gSF from particle-γ coincidence events and has been shown to be robust for a wide range of isotopes [17, 18, 19]. It is based on the Hauser-Feshbach model [20], where the formation and decay of the Compound nucleus are described independently, with the former based on optical model calculations, and the lat-

ter using statistical properties of the Compound nucleus. Finally, the σ(n,γ) cross section will be calculated using the experimental NLD and gSF as input to the Hauser-Feshbach type nuclear reaction simulation software TALYS [21]. Note that the Oslo method was initially applied to direct reaction kinematics using stable reaction targets but in recent years it has been also developed for inverse kinematics [22]. A successful experimental study using the ^{66}Ni(d,pγ)^{67}Ni reaction has been already performed at ISOLDE [23]. Data analysis via Oslo method has been finished and scientific paper is in preparation [24]
.

2 Experiment

We propose to measure the neutron particle-hole states of ^{80}Zn via single neutron transfer reaction ^{79}Zn (d,p) ^{80}Zn in inverse kinematics. The ^{79}Zn beam will be post-accelerated to an energy of 435 MeV (5.5 MeV/A), impinging on a 0.5 mg/cm^2 deuterated polyethylene CD_2 target. The target thickness is chosen to provide sufficient statistics for the analysis of both low- and high-energy γ rays and to reduce the uncertainty in the excitation energy due to the straggling in the target, important for the extraction of the NLD and gSF. A production yield of 1×10^6 ions at/μC for ^{79}Zn has been achieved using a UC_x target and laser ionized using RILIS [25] at the target position. However, the contamination from gallium isotopes is expected and thus purification of the beam can be necessary. We therefore consider a beam intensity of 1×10^5 pps for the yield estimation in the following.

The experimental setup will consists of the T-REX silicon-detector array [26] coupled to the MINIBALL γ-ray spectrometer [27]. This setup permits to detect the emitted protons in coincidence with the γ rays de-excited from the residual nucleus. The coincidence technique is necessary in the present case where the resolution of the proton spectra is limited due to the choice of the target thickness (0.5 mg/cm^2) and will allow us to resolve the states of interest. It has been already employed successfully by the previous studies at REX-ISOLDE. In addition, to increase the efficiency of detecting the higher energy γ rays for the Oslo method we propose to add 6 large volume $LaBr_3$ detectors by removing some of the MINIBALL detectors, as was done for the IS559 experiment [23].

None of the states of the multiplets $\nu 1g_{9/2}^{-1}\otimes\nu 2d_{5/2}^{1}$ in ^{80}Zn are known at present and will be selectively populated and identified by requiring an angular momentum transfer of $l=2$. The first excited 2^+ state at 1497 keV in ^{80}Zn is known from a Coulex experiment performed at ISOLDE [28]. The rest of the low-lying states are populated via a nucleon knockout reaction up to around 3.5 MeV at RIKEN [29]. However, none of the higher-lying states could be identified as $1p-1h$ multiplets. Figure 3a shows the level scheme of ^{80}Zn adopted from Ref. [29]. In order to estimate the cross sections of the final states via the (d,p) channel the Shell model predictions from Ref. [7] are used (Figure 3b). The calculations predicted the 5^+ and 6^+ states from 3.7 to 3.8 MeV with the $1p-1h$ excitations to the $2d_{5/2}$ orbital. Figure 3c shows the DWBA calculations performed for the $l=2$ transfer for the two states using the code FRESCO [30]. For the scattered protons from 20° to 50° in the laboratory frame, the cross sections of 95 and 60 mb are calculated for the $2d_{5/2}$ states at 3.7 and 3.8 MeV, respectively (for a spectroscopic factor of 1).

In addition, there will be other spin multiplets with 4^+ and 5^+ from the transfer of a

$(l = 0)$ neutron into the $3s_{1/2}$ orbit., i.e. the $\nu 1g_{9/2}^{-1} \otimes \nu 3s_{1/2}^{1}$ configuration. In the case of ^{80}Zn, the energy difference of the two orbitals $2d_{5/2}$ and $3s_{1/2}$ is expected to be less than ^{88}Sr $(Z = 38)$ primarily due to the lowering of the $3s_{1/2}$ state towards ^{80}Zn $(Z = 30)$. In fact, the energy difference between $1/2^+$ g.s. and $5/2^+$ state in the neutron-rich N=51 isotones was experimentally shown to decrease from 1.2 MeV in ^{91}Zr to 0.28 MeV in ^{83}Ge [31, 32]. Therefore, in order to estimate the reaction cross sections, the states of the $\nu 1g_{9/2}^{-1} \otimes \nu 2d_{5/2}^{1}$ are considered to lie 200 keV above the $\nu 1g_{9/2}^{-1} \otimes \nu 2d_{5/2}^{1}$ multiplets. The cross sections of 130 and 100 mb are calculated for the $3s_{1/2}$ states at 3.9 and 4 MeV, respectively, for the same range of the scattered protons mentioned above.

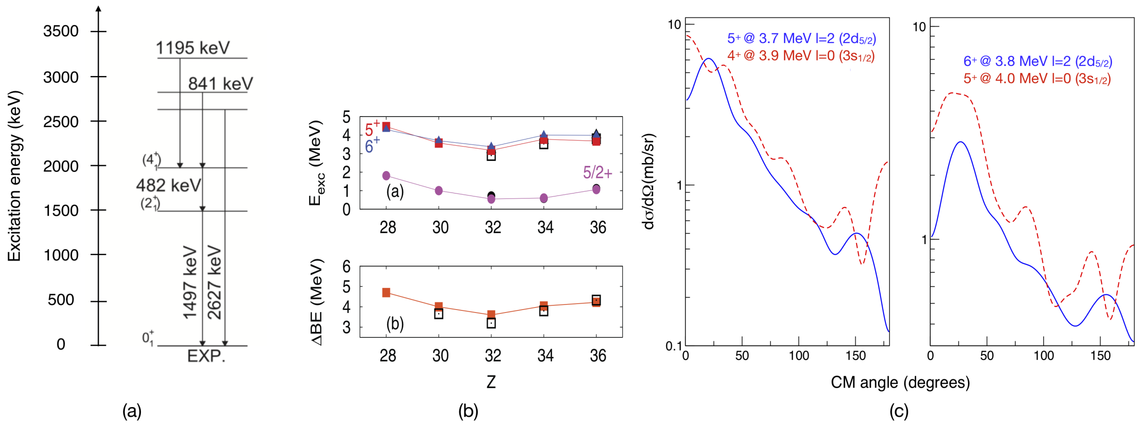

Figure 3: (a):Level scheme of ^{80}Zn (b):SM calculations of the 5^+, 6^+ states along the $N = 50$ isotones, taken from [7] (c):Angular distribution of protons emitted in the reaction populating the $2d_{5/2}$ states at 3.7 and 3.8 MeV(blue) and the $3s_{1/2}$ hypothetical states at 3.9 and 4 MeV (red).

With the given beam intensity and a target thickness of 0.5 mg/cm^2 the rates of about 1 and 1.4 events/sec are estimated for the states at 3.7 and 3.8 MeV, respectively. Proton detection efficiency in the barrel detector for both $2d_{5/2}$-character states is taken as 50% in a good approximation. The γ rays showing successive decays from $2d_{5/2}$ multiplets range from 250 keV to over 1.3 MeV for the other members of the isotonic chain. The absolute photo-peak efficiency of MINIBALL varies from 13% at 250 keV to 5% at 1.3 MeV.

For an average photopeak efficiency of 8%, final rates of:

- 3500 counts/day particle-γ and 290 counts/day particle-$\gamma\gamma$ coincidence events on average for each $2d_{5/2}$ state from 2^+ to 7^+
- 10000 counts/day particle-γ and 950 counts/day particle-$\gamma\gamma$ coincidence events for each $3s_{1/2}$ state (i.e. 4^+ and 5^+) are expected.

Note that particle-$\gamma\gamma$ coincidence data are particularly important in the present case in order to build a complete level scheme of ^{80}Zn. Therefore, in order to obtain a clear identification of the states of interest and the level scheme construction, we foresee a 6-day of data taking. Regarding the analysis of the statistical γ rays using the Oslo method, experience from the previous IS559 experiment shows that the expected level of statistics will be sufficient to extract the NLD and gSF, and use these quantities to constrain the (n,γ) cross section.

Summary of requested shifts: 18 shifts for the ^{79}Zn beam plus 3 shifts to optimize the production and purification of the beam.

References

[1] O. Sorlin and M.-G. Porquet, Prog. Part. Nucl. Phys. **61**, 602 (2008).

[2] A. Gottardo *et al.*, Phys. Rev. Lett. **116**, 182501 (2016).

[3] E. Sahin *et al.*, Nucl. Phys. A **893**, 1-12 (2012).

[4] C. R. Bingham *et al.*, Phys. Rev. C **2** 2297 (1970).

[5] K. K. Seth *et al.*, Phys. Rev. C **10** 1928 (1974).

[6] J. Prevost *et al.*, Eur. Phys. J. A **22**, 391 (2004) and references therein.

[7] K. Sieja and F. Nowacki, Phys. Rev. C **85** 051301(R) (2012).

[8] K.-L. Kratz *et al.*, Astrophys. J. 403, 216 (1993).

[9] R. L. Gill *et al.*, Phys. Rev. Lett. 56, 1874 (1986).

[10] S. Baruah *et al.*, Phys. Rev. Lett. **101**, 262501 (2008).

[11] J.J. Cowan *et al.*, Stars, Metal-Poor Stars, and the Galaxy, Carnegie Observatories Astro.Series Vol.5 (2011).

[12] M. Aoki *et al.*, Proc. 14th Int. Symp. on Nucl. in the Cosmos (NIC2016) JPS Conf. Proc. 14, 020302 (2017).

[13] R. Surman *et al.*, AIP Advances 4, 041008 (2014).

[14] M.R. Mumpower, R. Surman*et al.*, Prog. Part. Nucl. Phys. 86 (2016) 86-126.

[15] Y.-Z. Qian and S. E. Woosley, Astrophys. J 471, 331 (1996).

[16] R. Surman, G. C. McLaughlin, and W. R. Hix, Astrophys. J 643, 1057 (2006).

[17] A. Schiller et al., Nucl. Instrum. Methods Phys. Res. A **447**, 494 (2000).

[18] A. C. Larsen *et al.*, Phys. Rev. C **83**, 034315 (2011) and references therein.

[19] B.V.Kheswa *et al.*, Phys. Letts. B **744**, 268 (2015).

[20] Hauser, W., and H. Feshbach, 1952, Phys. Rev. 87, 366.

[21] A. Koning, S. Hilaire, M. Duijvestijn, TALYS: Nuclear Reaction Simulator. URL: https://tendl.web.psi.ch/tendl 2019/talys.html.

[22] V.W. Ingeberg *et al.*, Eur. Phys. J. A **56**, 68 (2020).

[23] S. Siem, M. Wiedeking et al., IS559 experiment.

[24] V.W. Ingeberg *et al.*, to be submitted.

[25] B. A. Marsh *et al.*, Hyperfine Interactions Vol. 196, 129 (2010).

[26] V. Bildstein *et al.*, Eur. Phy. Journ A. **48**, 85 (2012).

[27] J. Eberth *et al.*, Eur. Phys. J. A**20** (2004) 65.

[28] J. Van de Walle *et al.*, Phys. Rev. Lett. 99, 142501 (2007).

[29] Y. Shiga *et al.*, Phys. Rev. C **93** 024320 (2016).

[30] I. J. Thompson, Comput. Phys. Rep. **7**, 167 (1988).

[31] J.S. Thomas, Ph.D. Thesis, Rutgers University, 2005.

[32] J.S. Thomas *et al.*, Phys. Rev. C **76** 044302 (2007).

Appendix

DESCRIPTION OF THE PROPOSED EXPERIMENT

The experimental setup comprises: (*name the fixed-ISOLDE installations, as well as flexible elements of the experiment*)

Part of the	Availability	Design and manufacturing
(MINIBALL + T-REX)	☒ Existing	☒ To be used without any modification
[6 $LaBr_3$(Ce) detectors	☐ Existing	☐ To be used without any modification ☐ To be modified
	☒ New	☐ Standard equipment supplied by a manufacturer ☐ CERN/collaboration responsible for the design and/or manufacturing
[Part 2 of experiment/ equipment]	☐ Existing	☐ To be used without any modification ☐ To be modified
	☐ New	☐ Standard equipment supplied by a manufacturer ☐ CERN/collaboration responsible for the design and/or manufacturing
[insert lines if needed]		

HAZARDS GENERATED BY THE EXPERIMENT (if using fixed installation:) Hazards named in the document relevant for the fixed [MINIBALL + only CD, MINIBALL + T-REX] installation.

Additional hazards:

Hazards	[Part 1 of experiment/ equipment]	[Part 2 of experiment/ equipment]	[Part 3 of experiment/ equipment]
Thermodynamic and fluidic			
Pressure	[pressure][Bar], [volume][l]		
Vacuum			
Temperature	[temperature] [K]		
Heat transfer			
Thermal properties of materials			
Cryogenic fluid	[fluid], [pressure][Bar], [volume][l]		
Electrical and electromagnetic			
Electricity	[voltage] [V], [current][A]		
Static electricity			
Magnetic field	[magnetic field] [T]		
Batteries	☐		

Capacitors	☐		
Ionizing radiation			
Target material [material]	CD2		
Beam particle type (e, p, ions, etc)	^{79}Zn		
Beam intensity	10^6 pps		
Beam energy	5.5 MeV/u		
Cooling liquids	liquid N_2		
Gases	[gas]		
Calibration sources:	☐		
• Open source	☐		
• Sealed source	☐ Standard γ-ray source for MINIBALL [ISO standard]		
• Isotope			
• Activity			
Use of activated material:			
• Description	☐		
• Dose rate on contact and in 10 cm distance	[dose][mSV]		
• Isotope			
• Activity			
Non-ionizing radiation			
Laser			
UV light			
Microwaves (300MHz-30 GHz)			
Radiofrequency (1-300 MHz)			
Chemical			
Toxic	[chemical agent], [quantity]		
Harmful	[chem. agent], [quant.]		
CMR (carcinogens, mutagens and substances toxic to reproduction)	[chem. agent], [quant.]		
Corrosive	[chem. agent], [quant.]		
Irritant	[chem. agent], [quant.]		
Flammable	[chem. agent], [quant.]		
Oxidizing	[chem. agent], [quant.]		
Explosiveness	[chem. agent], [quant.]		
Asphyxiant	[chem. agent], [quant.]		

Dangerous for the environment	[chem. agent], [quant.]		
Mechanical			
Physical impact or mechanical energy (moving parts)	[location]		
Mechanical properties (Sharp, rough, slippery)	[location]		
Vibration	[location]		
Vehicles and Means of Transport	[location]		
Noise			
Frequency	[frequency],[Hz]		
Intensity			
Physical			
Confined spaces	[location]		
High workplaces	[location]		
Access to high workplaces	[location]		
Obstructions in passageways	[location]		
Manual handling	[location]		
Poor ergonomics	[location]		

Hazard identification:

Average electrical power requirements (excluding fixed ISOLDE-installation mentioned above): [make a rough estimate of the total power consumption of the additional equipment used in the experiment]: ... kW